High quality beam shaping by square soft-edge diaphragm combined with liquid crystal spatial light modulator

Yunfeng Ma (麻云凤)[1,2,3], Zhongwei Fan (樊仲维)[1,3*], Jisi Qiu (邱基斯)[1,2,3], Chengyong Feng (冯承勇)[1,2,3], Tianzhuo Zhao (赵天卓)[1,2,3], and Weiran Lin (林蔚然)[1]

[1] *The Academy of Opto-Electronics, Chinese Academy of Sciences, Beijing 100080, China*

[2] *Graduate University of Chinese Academy of Sciences, Beijing 100049, China*

[3] *Beijing GK Laser Technology Co., Ltd, Beijing 100085, China*

[*] *E-mail: fanzw002@163.com*

Received April 29, 2009

The square soft-edge diaphragm with round angle is designed by Matlab, and is sent to a liquid crystal spatial light modulator by the computer. In order to obtain precompensation for the following laser system, local diaphragm transmission can be adjusted by feedback signals of surface-channel charge-coupled device (SCCD). This method can reduce the diffraction effect and realize no modulation, high stability, high homogeneity, and large scale laser beam. Several parameters of soft-edge diaphragms which affect the laser beam quality are studied systematically, and the optimized values are obtained. The method can avoid the serious modulation of hard edges and provide soft-edge diaphragms of different shapes in a fast and convenient way for the large scale laser beam system.

OCIS codes: 050.1220, 140.3300, 230.3720.

doi: 10.3788/COL20100802.0134.

High power and high brightness lasers have wide applications in industry, military, and everyday life. The methods to obtain large scale, high stability, high homogeneity, and high power lasers have attracted more and more attention in recent years[1−3].

Generally, in order to obtain the large scale laser beam with high homogeneity, high intensity, and no ghost point, formally, the laser is first extended by extender lens, then, it is shaped by a diaphragm, and finally, it is filtered by a spatial filter. So the large scale laser can reach the demands of high quality[4]. There are several diaphragms for shaping. For example, hard-edge diaphragm, saw-tooth diaphragm, etc.[5−7] However, these diaphragms induce seriously high frequency components which affect the large scale laser beam quality. And the conventional methods of making diaphragms include photoetching, coating, machine processing, etc. Once these diaphragms are made, their shapes cannot be changed at will. Simultaneously, all methods do not make high-quality soft-edge diaphragms and the transmission is not adjustable.

Recently, the liquid crystal spatial light modulator (LC-SLM) is used to shape the phase and amplitude[8]. The advantage of the LC-SLM is that the shape of the diaphragm is adjustable randomly by Matlab, and the transmission and phase can be adjusted by gray scale control of the image by feedback signals[9]. Chen *et al.* proposed an idea of large scale laser shaping by the LC-SLM[10]. Qin *et al.* reported square laser beam shaping, by which the high frequency component is always easier to be erased through a spatial filter[11].

Nevertheless, the systemic square soft-edge diaphragm with round angle has not yet been reported, which is introduced in detail in this letter including mathematical model. The soft-edge diaphragm was designed at the wavelength of 1064 nm and two key parameters of soft-edge diaphragm were also discussed in our experiment.

It is well known that the sharp angle and hard edge induce serious modulation inside the large scale laser beam[12−13]. So the diaphragm is designed with a soft edge and four round angles. The process of design is as follows.

1) Set up Gamma curve

Since different gray scales have different transmissions at 1064 nm, images of 0–255 red-green-blue (RGB) values are imported into the computer through a video graphics array (VGA) data line. The images are made for a step of every 5 RGB values, by which the transmission values are calculated and Gamma curve is plotted in Fig. 1.

The results show that the behavior strongly depends on the polarizer used. A better polarizer (1000:1) will enhance the contrast (200:1) at 1064 nm. By virtue of the Gamma datum, the soft-edge diaphragm is designed by Matlab.

2) Design soft-edge diaphragm image

The LC-SLM shows serious diffraction effect and low transmission of electrode plates. These effects produce edge effect and energy loss which result in a duty ratio of only 55% with a transmission of 20%. According to the Gamma datum, the soft-edge diaphragm image is made

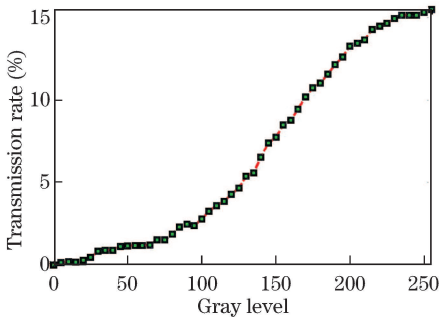

Fig. 1. Amplitude modulation curve which is called Gamma curve.

 © 2010 Chinese Optics Letters

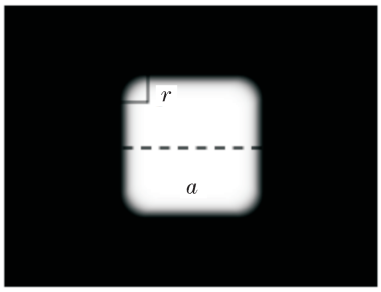

Fig. 2. Soft edge diaphragm image.

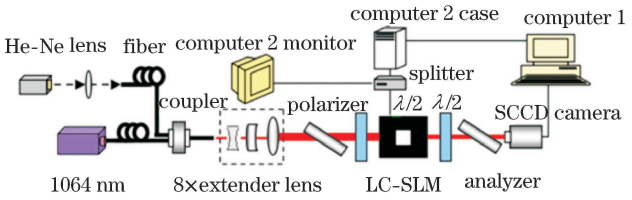

Fig. 3. Experimental setup for the soft edge diaphragm by amplitude modulation method.

by Matlab as shown in Fig. 2. The whole soft-edge diaphragm image has a size of 832×624 pixels.

The distribution of the RGB value intensity is a super-Gaussian profile. The expressions are as follows:

$$\begin{cases} I(x,y) = I_0 \exp[-(x/g_1)^{2N}], & k \le 1-2C, \\ I(x,y) = I_0 \exp[-(y/g_1)^{2N}], & k \ge 1-2C, \\ I(x,y) = I_0 \exp[-(\sqrt{x^2+y^2}/g_2)^{2N}], & \\ \text{others and } x,y \le a-2r, & \end{cases} \tag{1}$$

where I_0 denotes the amplitude constant, $I(x,y)$ is the intensity function of RGB value, a represents the side length, N is the Gauss number, x,y are the Cartesian coordinates r is the round angle radius, $k = y/x$ is a ratio, $C = r/a$ is a round angle ratio, and $g_1 = (a-1)(-\ln 0.01)^{2N}/2$, $g_2 = \sqrt{x^2+y^2}(-\ln 0.01)^{2N}$, while $x,y \le a-2r$.

Figure 3 shows the experimental setup for the laser beam shaping by amplitude modulation.

A twisted-nematic LC-SLM (LC2002, Holoeye, Germany) is used in the experiment. In this device, about 10-μm nematic liquid crystal is sandwiched between two layers of transparent electrode plates (with a transmission higher than 90%). Accordingly, the long axes of liquid crystal molecules continuously twist 90° between these two plates. By virtue of a VGA data line, the computer gray image is imported into the LC-SLM and the transmission can be controlled. The LC-SLM is composed of 832×624 pixels and the pixel pitch is 32 μm. The LC-SLM is worked at the voltage of 15 V, and refreshed at the rate of 60 Hz, 256 colors, and 8 bits, which is set by the computer 2. In order to avoid long electric heating and laser radiation, the LC-SLM is set up an electronic control translation stage which is controled by computer 1. The LC-SLM is removed every 20 min, and the power is shut off automatically.

In order to reshape the laser beam and provide a precompensation for the following systems, the gray image signals on the computer screen are sent to the LC-SLM, and the near field optical pattern is guided to the surface-channel charge-coupled device (SCCD) camera (Spiricon LBA-usb-L230 with 1616×1216×8 bits) which is controlled by computer 1. computer 2 case simultaneously controls computer 2 monitor and the LC-SLM through a splitter. Two main functions can be realized by computer 2, i.e., importing gray images into the LC-SLM and controlling the transmission through computer 1 by SCCD feedback signals. This design is able to offer precompensation for the following systems, for example, compensating the optical system modulation caused by dust and defect points from the imperfect surface of optical elements.

As depicted in Fig. 3, a Nd:YVO_4 laser is used as a light source and a He-Ne laser is used as a guide for optical alignment. Both the infrared (1064 nm) and red (632.8 nm) beams are coupled into the 8×extender lens through the coupler. The 8×extender lens, designed by Zemax, conform to Fourier transfer function with no aberration. After the expansion, the infrared laser beam has a diameter of 10 mm (Φ10 mm) and passes in sequence through the polarizer, the half wave plate (HWP), the LC-SLM, and the other HWP.

In our experiment, the LC-SLM shows the highest transmission while the 1064-nm beam has an initial linear polarization angle of about 45°, which is offered by the polarizer and the HWP. The LC-SLM rotates this polarization to 135°. At the exit of the LC-SLM, the HWP rotates this from 135° to 0° again, which means a horizontally polarized beam is produced. The output beam then passes the analyzer.

For the 10-mm beam with 10-mm diameter, the whole transmission is 12% without the HWP. And this rate is increased to 15.6% while the HWP is inserted in the system. The enhancement can be explained by the fact that the LC-SLM has an initiative polarization angle for different wavelengths, which is proved to be 45° at 1064 nm in our experiment. And it is also noticed that for 3-ns pulses, the damage threshold of LC-SLM is around 10 mJ/cm^2.

This soft-edge diaphragm is designed to reduce the serious diffraction effects always connected with the hard-edge of diaphragms. In order to get a comprehensive evaluation of our soft-edge diaphragms, all the measurements are performed with the same system Fresnel number, which is given by $F = a^2/\lambda L$, where a is the side length of diaphragm, λ is the wavelength, and L is the propagation distance of light.

When $F = 84.9$ ($a = 4.25$ mm, $\lambda = 1064$ nm, $L = 200$ mm), the images of the diaphragm with different Gaussian numbers are imported into computer 2, and the optical images are collected by SCCD. All images have a C value of 0.175 (C is the round angle ratio). Figure 4 shows the collected optical spots with Gaussian number $N = 1, 2, \cdots, 9$.

Some formulas are built to analyze the characteristics of the above images. Small-scale contaminants or optics imperfections lead to beam intensity modulations. At high intensity, these modulations are amplified and focused by the nonlinear index effect. An early sign of the development of this instability grows in the beam contrast. Fluence beam contrast

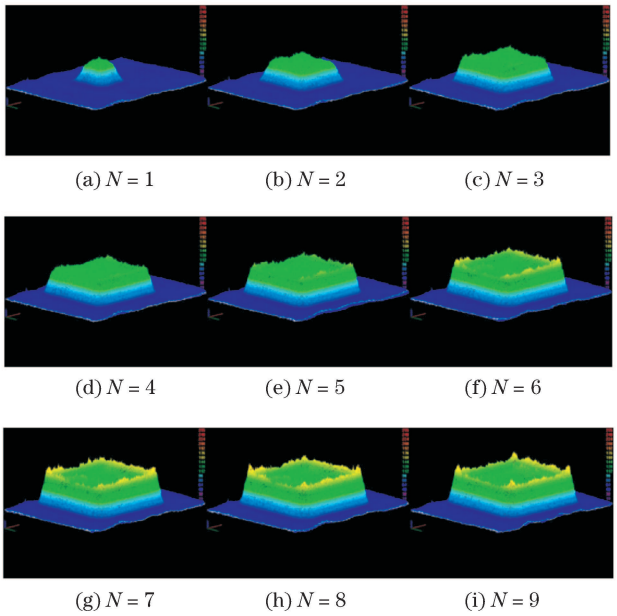

Fig. 4. Collected optical spots with different Gaussian numbers.

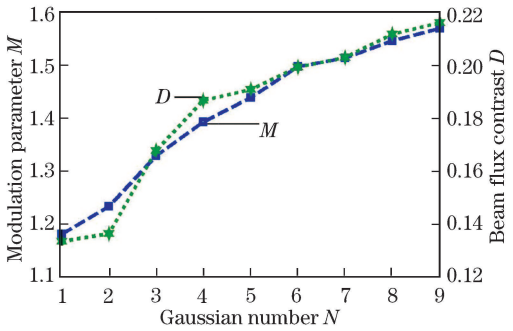

Fig. 5. Modulation parameter M and fluence beam contrast D with Gaussian number $N = 1, 2, \ldots, 9$.

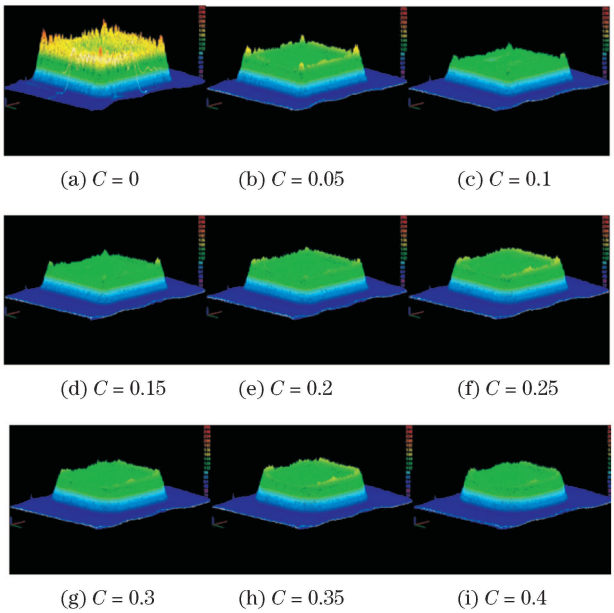

Fig. 6. Collected optical images with $C = 0, 0.05, 0.1, \cdots, 0.4$.

describes median and high frequency optical intensity modulation which are result from small-scale self-focusing[3,12]. And fluence beam contrast is defined as $D = 1/I_{\text{avg}} \sqrt{\sum_{i=1}^{m} \sum_{j=1}^{n} [I(x_i, y_j) - I_{\text{avg}}]^2/(\text{nm})}$, where $I(x_i, y_j)$ is the pixelated fluence from near-field SCCD image, I_{avg} is the average fluence of image, i and j are the numbers of pixelated fluence datum, ranging from 1 to m and n, respectively.

The optical intensity modulation parameter is defined as $M = I_{\max} / I_{\text{avg}}$, in which $I_{\max}$ and I_{avg} are the maximum and average values of optical intensities, respectively. The datum analyses of Fig. 4 are shown in Fig. 5. It is obvious that the modulation parameter M and the fluence beam contrast D increase with the increase of Gaussian numbers.

The experimental results show that the right angle in the diaphragm results in serious diffraction patterns with $M = 1.58$ and $D = 0.218$. In order to reduce this diffraction, round angles need to be used in soft-edge diaphragms.

When $F = 84.9$, the images with different round angle ratios are imported into computer 2, and the optical images are designed with $N = 7$. Figure 6 shows the different values of C from 0 to 0.4.

Figure 6 tells that the laser beam is most seriously diffracted when the round angle ratio C is 0 (right angle). And high modulation is introduced into the inner region. Figure 7 shows that M and D decrease with increasing C. When C ranges from 0.05 to 0.25, the modulation decreases gradually, and the square shape is kept. When C ranges from 0.3 to 0.4, the shape changes from square to circle, and M is close to the constant of 1.45. When C equals 0.5, the shape is circle.

The fill factor of laser beam can be defined as $F_{\text{beam}} = S_{90\%I} / S_{1\%I}$, where $S_{90\%I}$ and $S_{1\%I}$ are the areas of 90% and 1% of the optical intensity values, respectively. When C and N equal 0.25 and 5 respectively, the range of this fill factor is $0.7 \leq F_{\text{beam}} \leq 0.9$, M is calculated to be 1.2, and D equals 0.15. Due to the edge effect of the LC-SLM, the diaphragm has an optimal size of less than 80% of liquid crystal size. The transmission of 4.25×4.25 (mm) diaphragm is 3%. The values of the two parameters are designed with specific requirements.

With the purpose of obtaining no modulation, high stability, high homogeneity, and large scale laser beam, Matlab is utilized to offer flexible soft-edge diaphragm.

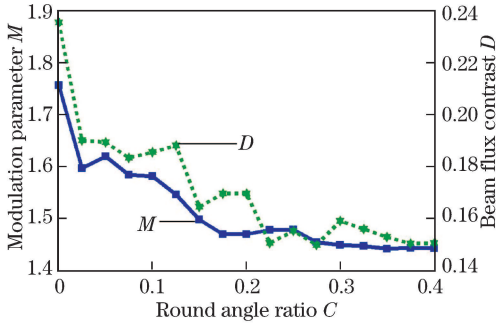

Fig. 7. Modulation parameter M and fluence beam contrast D with circle angle ratio C range from C=0, 0.025, 0.05, $\cdots$, 0.4.

Combining with feedback signal from computer 1, computer 2 modulates local RGB values of soft-edge diaphragm to adjust the local transmission, through which laser beam obtains precompensation for the following optical systems. Although the whole system transmission is smaller than that of etching diaphragm, it is worth losing a part of power to get an excellent quality laser beam for the following main amplifier system.

In conclusion, we introduce a technology of square soft-edge diaphragm with four round angles. It is designed by Matlab combined with the LC-SLM. The design can reduce the diffraction effect and realize a high beam quality for the large scale laser system. The method offers automatic and flexible optical design, which can realize the precompensation for the following optical systems. Simultaneously, the highest transmission is obtained by this optical design. By virtue of a number of experiments, several diaphragm parameters which influence the laser beam quality are studied systematically. The best round angle ratio and Gaussian number which keep high-quality square laser beam are obtained. This method of optical design has been practically realized and found great advantage in our preamplifier modules system.

This work was supported by the National "863" Program of China under Grant Nos. 2007AA03Z448 and 2008AA031901.

References

1. V. I. Annenkov, V. G. Bezuglov, A. V. Bessarab, Y. D. Bogunenko, G. A. Bondarenko, I. V. Galakhov, S. G. Garanin, N. V. Zhidkov, S. V. Kalipanov, N. A. Kalmykov, V. P. Kovalenko, S. G. Lapin, S. L. Logutenko, V. M. Murugov, V. A. Osin, V. I. Pankratov, M. Y. Romashov, A. V. Ryadov, V. A. Starodubtsev, R. R. Sungatullin, V. S. Faizullin, V. A. Khrustalev, N. M. Khudikov, and V. S. Chebotar', Quantum Electron. **36,** 508 (2006).
2. S. E. Bodner, Appl. Opt. **47,** 1387 (2008).
3. C. A. Haynam, P. J. Wegner, J. M. Auerbach, M. W. Bowers, S. N. Dixit, G. V. Erbert, G. M. Heestand, M. A. Henesian, M. R. Hermann, K. S. Jancaitis, K. R. Manes, C. D. Marshall, N. C. Mehta, J. Menapace, E. Moses, J. R. Murray, M. C. Nostrand, C. D. Orth, R. Patterson, R. A. Sacks, M. J. Shaw, M. Spaeth, S. B. Sutton, W. H. Williams, C. C. Widmayer, R. K. White, S. T. Yang, and B. M. V. Wonterghem, Appl. Opt. **46,** 3276 (2007).
4. C. Wang, S. Chen, F. Xu, X. Xie, X. Ge, S. Xu, Z. Lin, D. Fan, and X. Deng, Chin. J. Quantum Electron. (in Chinese) **17,** 479 (2000).
5. Y. Rao, S. Xu, S. Meng, and Z. Lin, Acta Opt. Sin. (in Chinese) **15,** 931 (1995).
6. W. Ge, Y. Liu, S. Ma, and B. Lv, Laser J. (in Chinese) **26,** 48 (2005).
7. L. M. Vinogradsky, V. A. Kargin, S. K. Sobolev, I. G. Zubarev, M. V. Pyatakhin, Y. V. Senatsky, A. V. Shelobolin, V. M. Mizin, and K. Ueda, Proc. SPIE **3889,** 849 (2000).
8. J. Kang, W. Zhang, H. Wei, S. Chen, and J. Zhu, Chin. Opt. Lett. **4,** 184 (2006).
9. J. Arines, V. Duran, Z. Jaroszewicz, J. Ares, E. Tajahuerce, P. Prado, J. Lancis, S. Bara, and V. Climent, Opt. Express **15,** 15287 (2007).
10. H. Chen, Z. Sui, Z. Chen, Bo An, and M. Li, Acta Opt. Sin. (in Chinese) **21,** 1107 (2001).
11. Y. Qin, X. Tang, R. Zhong, and Z. Li, Proc. SPIE **6825,** 68250W (2007).
12. S. P. Anokhov, R. A. Lymarenko, and A. I. Khizhnyak, Radiophys. Quantum Electron. **47,** 926 (2004).
13. J. Gu, D. Zhao, Z. Mei, and H. Mao, Optik **115,** 337 (2004).